

# Anomalous anisotropic magnetoresistance in epitaxial $\text{Fe}_3\text{O}_4$ thin films on $\text{MgO}(100)$

R. Ramos\*, S. K. Arora, and I. V. Shvets

*Centre for Research on Adaptive Nanostructures and Nanodevices (CRANN),*

*School of Physics, Trinity College Dublin, Dublin 2, Ireland*

(Dated: 22 October 2008)

## Abstract

Studies of the angular dependence of the anisotropic magnetoresistance (AMR) are reported for epitaxial films of magnetite ( $\text{Fe}_3\text{O}_4$ ) grown on  $\text{MgO}$  (001) and also for single crystals of magnetite. The characteristic feature of the AMR is a two-fold symmetry at temperatures above 200 K. As the samples are cooled below 200 K, an additional set of peaks appears. These become dominant at lower temperatures showing an overall four-fold symmetry. Observation of additional anisotropy in the AMR points to formation of charge ordering at much greater temperatures than the Verwey transition temperature and is possibly related to the polaron formation in magnetite.

PACS numbers: 75.47.-m, 75.50.Bb, 71.30.+h

## I. INTRODUCTION

Many transition metal oxides exhibit charge and orbital ordering which manifests itself in a spatial localization of charge carriers on certain ionic sites and electron orbitals, respectively. These correlated ordering processes govern the physical properties, such as; magnetism and charge transport, and are responsible for many ubiquitous phenomena.<sup>1-3</sup> Magnetite,  $\text{Fe}_3\text{O}_4$ , is one of the important 3d transition metal oxides, due to its half metallic nature, high Curie temperature (858 K) and presence of a metal-insulator transition (MIT) at around 121 K (known as Verwey transition). Hence, it is viewed as a potentially interesting material for spintronic applications.<sup>4,5</sup> The Verwey transition in  $\text{Fe}_3\text{O}_4$  leads to a change in conductivity by two orders of magnitude across the transition temperature and is believed to be associated with a order-disorder transition from a charge-ordered state of B-site Fe ions ( $\text{Fe}^{+2,+3}$ , for octahedral Fe-ions) at low temperatures to a disordered state ( $\text{Fe}^{+2.5}$  at all B-sites) at higher temperatures. Despite decades of activity, the underlying physics related to this transition is not yet completely clear.<sup>6</sup> Various techniques have been used to grow epitaxial hetero-structures based on magnetite. MgO is an ideal template to grow  $\text{Fe}_3\text{O}_4$  films owing to the small lattice mismatch.<sup>7-10</sup> However, the  $\text{Fe}_3\text{O}_4/\text{MgO}$  hetero-epitaxial system suffers from the formation of antiphase boundaries (APB) which is an innate outcome of the growth process due to the fact that  $\text{Fe}_3\text{O}_4$  has a unit cell which is twice the size and lower in symmetry compared to MgO.<sup>7-10</sup> The presence of APBs has a deleterious effect on the magnetic properties but they are beneficial in enhancing the magneto-resistance of films due to additional spin scattering they induce.<sup>11,12</sup> Magneto-transport studies in epitaxial magnetite films are mostly focused on the influence of APBs, disorder and strain. In a recent study,<sup>13</sup> we have shown that if these nano-scale defects in  $\text{Fe}_3\text{O}_4$  films are manipulated in an ordered fashion one can attain a sizable magnetoresistance.

Understanding mechanisms that affect the magneto-transport behavior in  $\text{Fe}_3\text{O}_4$  is of crucial importance in realization of its application as a magneto-resistive sensor. One of the mechanisms contributing to the magneto-transport phenomenon is the anisotropic magneto-resistance, AMR. In ferromagnets, the AMR is caused by the spin-orbit interaction, which induces the mixing of spin-up and spin-down states.<sup>14-16</sup> This mixing depends on the magnetization direction and gives rise to a magnetization-direction dependent scattering rate. As a result, the conductivity of a saturated sample is affected by the angle between the

electrical current  $\vec{J}$  and magnetization  $\vec{M}$ . The angular dependence of resistivity is given by

$$\rho = \rho_{\perp} + (\rho_{\parallel} - \rho_{\perp})\cos^2\theta \quad (1)$$

Where  $\rho_{\parallel}$  and  $\rho_{\perp}$  are the resistivities for  $\vec{M} \parallel \vec{J}$  and  $\vec{M} \perp \vec{J}$  respectively. Various mechanisms have been proposed to explain the origin of the AMR and its link to spin-orbit coupling. Some aspects of AMR have been dealt theoretically by Smit,<sup>14</sup> Berger,<sup>17</sup> Potter,<sup>18</sup> Campbell and Fert.<sup>19</sup> In ferromagnetic poly crystalline alloys the magnitude of the AMR is around 20 and 5 % at low temperature (20 K) and room temperature respectively. In thin films, its magnitude is further reduced due to surface scattering and additional structural effects. In single crystals and epitaxial thin films, in contrast to poly-crystals, additional features in AMR at low fields are observed which are related to the magneto-crystalline anisotropy and the AMR exhibits a deviation of the angular dependence from the  $\cos^2\theta$  curve.<sup>20,21</sup> Enhanced magnitude of up to several tens of percent could be obtained in nano-structured devices like multilayers, constrictions in the ballistic regime, and nano-wires.<sup>22,23</sup> There are studies aimed at understanding the charge and spin coupling on AMR. In particular, AMR investigations in epitaxial thin films and single crystals of rare earth manganites have shown an anomalous temperature dependence where the magnitude of AMR peaks at a temperature close to the MIT, which is an issue actively debated by theoreticians and experimentalists.<sup>24,25</sup> In  $\text{Fe}_3\text{O}_4$  films, the AMR investigations have been performed by Ziese et al.<sup>26</sup> In films of thickness larger than 15 nm, they found a temperature independent AMR ( $\sim 0.5$  %) for  $T > 200\text{K}$ , and a sign change in AMR at temperatures close to Verwey transition. No details of the angular dependence of the AMR were provided.

In this paper we report a detailed study of angular and temperature dependence of AMR in a synthetic single crystal of  $\text{Fe}_3\text{O}_4$  and epitaxial  $\text{Fe}_3\text{O}_4$  films of different thickness grown on MgO (001) substrates. Remarkably, in angular dependence of AMR, we observe an additional anisotropy, superimposed on the conventional two-fold anisotropy at temperature below 200 K. Its magnitude grows with an increasing field and decreasing temperature. We provide possible explanations for the observed effect.

## II. EXPERIMENTAL

The  $\text{Fe}_3\text{O}_4$  thin films of thicknesses 33, 67 and 200 nm were grown on MgO (001) single crystal substrates using an oxygen plasma assisted molecular beam epitaxy (DCA MBE M600) with a base pressure of  $5 \times 10^{-10}$  Torr. The substrates were annealed at  $600^\circ\text{C}$  in UHV for 1/2 h followed by 2 h annealing in  $1.1 \times 10^{-5}$  Torr oxygen. The growth of  $\text{Fe}_3\text{O}_4$  films was carried out by means of electron beam evaporation of pure metallic Fe (99.999 %) in the presence of free oxygen radicals ( $1.1 \times 10^{-5}$  Torr). Substrate temperature during growth was  $250^\circ\text{C}$ . Details of the growth procedure can be found elsewhere.<sup>13</sup> Resistance versus temperature measurements for the samples were performed using a standard four probe method. Prior to the transport measurements, the samples were patterned into the Hall bar geometry by UV-lithography and chemically etched with an 8.55 M HCl solution. The magneto-transport measurements were carried out using a Physical Property Measurement System (PPMS 6000 system of Quantum Design), which is equipped with a 14 T superconducting magnet and a sample rotator to perform the measurements at different field orientations in a temperature range of 2-400 K. In order to study the angular dependence of the AMR, the samples were subjected to a constant in-plane magnetic field  $\vec{H}$ , while the angle  $\theta$ , with respect to the electric current  $I$ , was changed from 0 to 360 degrees. The longitudinal voltage which is proportional to the AMR was measured between contacts  $V^+$  and  $V^-$  (inset Fig. 2(a)). A DC bias current was applied along the  $\langle 100 \rangle$  direction, the applied current was always kept in 1-10  $\mu\text{A}$  range for the thin film samples and in 1-10 mA range for the single crystal, the I-V characteristics of the studied samples exhibited linear behavior for the electrical currents used in the AMR experiment, for all the temperatures measured. The synthetic crystal of  $\text{Fe}_3\text{O}_4$  used in this study was grown employing the skull melting technique and showed a Verwey transition temperature of 119 K.

## III. RESULTS AND DISCUSSION

We present a systematic study of the angular dependence of the anisotropic magnetoresistance at different temperatures and magnetic field strengths on 33, 67 and 200 nm thick  $\text{Fe}_3\text{O}_4$  films grown on MgO(001) substrates. Prior to the AMR measurements the temperature dependence of the resistivity was measured. Figure 1(a) shows the resistivity as a function of

temperature for all the films. Also shown in the figure is the data for a single crystal slice of  $\text{Fe}_3\text{O}_4$  cut along the (001) plane. Resistivity of the films at 300 K is found to increase with a decrease in film thickness and is greater than that of the single crystal. Verwey transition temperature ( $T_V$ ) for 33, 67 and 200 nm films is found to be 110, 112 and 121 K respectively. These observations are in line with the previously reported values of resistivities and  $T_V$ .<sup>26,27</sup> Temperature dependence of resistivity for  $\text{Fe}_3\text{O}_4$  films suggests that the electronic transport in  $\text{Fe}_3\text{O}_4$  follows a thermally activated behaviour. As previously reported,<sup>28</sup> three regions with different activation energies can be distinguished. The first one is a high temperature region ( $T \gtrsim 200$  K), the second is a middle temperature region (just above  $T_V$  up to  $\sim 200$  K) and the third a low temperature region (below  $T_V$ ), hereafter referred to as region I, II and III respectively. In order to understand the mechanism of charge transport in  $\text{Fe}_3\text{O}_4$ , we fitted the resistivity data using expressions for small-polaron hopping ( $\rho/T^{3/2} = A\exp(W_p/k_B T)$ ) in region I, Arrhenius law or band gap model ( $\rho = \rho_\infty \exp(E_a/k_B T)$ ) in regions II and III and variable-range hopping ( $\rho = \rho_\infty \exp(T_0/T)^{1/4}$ ) for temperatures below  $T_V$ .<sup>29</sup> Figures 1(b) to 1(d) show the data for the 67 nm thick film fitted to small-polaron hopping (Fig. 1(b)), Arrhenius law (Fig. 1(c)) and variable-range hopping (Fig. 1(d)). From the slope of the curves we obtain the polaron hopping energy ( $W_p$ ), activation energy ( $E_a$ ) and Mott temperature ( $T_0$ ) respectively. These parameters obtained using the above models are summarized in Table I. The values of  $E_a$  agree well with previous reports<sup>26</sup> both above and below  $T_V$ . The Mott temperature  $T_0$  is found to be related to the localization length<sup>30</sup> and agrees well with earlier reported values.<sup>31</sup> The existence of two different electrical conduction regions above  $T_V$  (*i. e. region I and II*) in magnetite agrees well with the Ihle et al.'s model<sup>32</sup> for small polaron (SP) band and SP hopping conduction, the first one being dominant at lower temperatures (just above  $T_V$ , region II) and the latter one at higher temperatures (region I).

Now, let us examine the temperature and magnetic field dependence of the measured AMR. The AMR is usually defined as the ratio:  $\text{AMR} = (\rho_{\parallel} - \rho_{\perp})/\rho_{ave}$ , where  $\rho_{\parallel}$ ,  $\rho_{\perp}$  are the resistivities for magnetic field applied parallel, perpendicular to the current direction respectively and  $\rho_{ave} = \rho_{\parallel}/3 + 2\rho_{\perp}/3$ . Our results show a room temperature value of about 0.3 %, in agreement with earlier reports.<sup>26,33,34</sup> Figure 2(a) shows the relative amplitude of the angular dependence of the magnetoresistance for the 67 nm sample at an applied field of 5 Tesla for a series of temperatures  $T = 300, 250, 200, 150, 120$  K (defined as:

$\Delta\rho/\rho_{min}(\%) = [(\rho(\theta) - \rho_{min})/\rho_{min}] * 100$ , where  $\theta$  is the angle between magnetic field and current and  $\rho_{min}$  is the minimum of resistivity for each scan). The data was also taken in the reverse angular sweep and resulted in no hysteresis in the AMR. At high temperatures (above 200 K), the angular dependence of AMR follows the typical  $\cos^2\theta$  dependence (two-fold symmetry) with peaks at  $0^\circ$  and  $180^\circ$  and valleys at  $90^\circ$  and  $270^\circ$  respectively. When the sample is cooled down to a temperature below 200 K a deviation from the two-fold symmetry starts to appear with the valleys near  $90^\circ$  and  $270^\circ$  broadening and eventually an additional set of peaks appearing showing an overall four-fold symmetry, which becomes dominant at lower temperatures. Similar behavior was exhibited by a (001) oriented stoichiometric  $\text{Fe}_3\text{O}_4$  single crystal (Fig. 2(b)). Similar features in the angular dependence of AMR have been previously observed in manganites<sup>35</sup> and more recently in diluted magnetic semiconductors (DMS).<sup>36,37</sup> In the latter case it has been related to the existence of two conduction mechanisms with different temperature dependencies. In general, additional anisotropy terms in the AMR response appear for single crystalline thin films provided the magnitude of external field is below the anisotropy field, such an example can be found for the case of a manganite thin film.<sup>38</sup> Besides the additional anisotropy terms arising from the magneto-crystalline anisotropy, they also observed appearance of hysteresis in angular dependence at small fields and low temperatures and attributed it to magnetic in-homogeneities.

The appearance of an additional anisotropy in the AMR in  $\text{Fe}_3\text{O}_4$  films is quite surprising. In order to establish its possible origin, we investigate the angular dependence of AMR at different magnetic fields. A representative data of angular scans for a 67 nm thick  $\text{Fe}_3\text{O}_4$  film measured at 150 K with varying magnetic field strengths (0.1, 0.5, 1.0, 5.0 and 14 Tesla) is shown in Fig. 3(a). Surprisingly, we notice that even with an increase in the magnetic field up to 14 T, we could not overcome this anisotropy. Furthermore the fact that the peaks related to the additional anisotropy are present at positions where the angle between the magnetic field and current is  $90^\circ$ , could suggest that it originates because of the contribution of Lorentz force (whose magnitude is greatest when the field is applied perpendicular to the current). The Lorentz force related contribution can be observed if  $\omega_c\tau > 0.1$ , where  $\omega_c$  is the cyclotron frequency ( $\omega_c = eB/m^*c$ ) and  $\tau$  is the scattering time. This condition can be written as  $BR_H/\rho = \tan\theta_H > 0.1$  where  $R_H$  is the Hall coefficient and  $\theta_H$  the Hall angle. For a 5 Tesla field we estimate a value of  $BR_H/\rho = \tan\theta_H \sim 10^{-5}$ , therefore, Lorentz force effects can be ruled out. Furthermore the magnetoresistance ( $\text{MR}(H)(\%) = [(\rho(H) - \rho(0))/\rho(0)] * 100$ ) of

the samples is always negative (see Fig. 3(b)), in contrast to the positive magnetoresistance expected from the Lorentz force effects.

In order to understand the mechanism related to this additional anisotropic terms in AMR behaviour of magnetite, we need to look at the details of the origin of AMR in ferromagnets. Phenomenologically, AMR shows a two-fold symmetry for polycrystalline materials because the magnetocrystalline effect is averaged out. However in single crystals and epitaxial films, it contains higher order terms which reflect the symmetry of the crystals.<sup>39,40</sup>

Using the phenomenological description for the anisotropic magnetoresistance, the dependence of the resistivity tensor with respect to the angle between magnetization and current can be calculated. Expanding the resistivity tensor as a function of the direction cosines of the magnetization and considering the symmetric part only gives:

$$\rho_{ij}(\vec{\alpha}) = a_{ij} + a_{ijkl}\alpha_k\alpha_l + a_{ijklmn}\alpha_k\alpha_l\alpha_m\alpha_n + \dots \quad (2)$$

where  $a_{ij}, a_{ijkl}, a_{ijklmn}$  are elements of the tensor up to the fourth order and the  $\alpha_k$  are the direction cosines of the magnetization. The number of coefficients can be reduced considering the Onsager relation ( $\rho_{ij}(\vec{\alpha}) = \rho_{ij}(-\vec{\alpha})$ ) and symmetry of the crystal<sup>41</sup>. For an in-plane magnetization and current applied in the  $\langle 100 \rangle$  direction, the obtained resistivity tensor looks as follows:

$$\rho(\theta) = C_0 + C_2\cos^2\theta + C_4\cos^4\theta \quad (3)$$

with  $C_0 = a_{11} + a_{1122} + a_{111122}$ ,  $C_2 = a_{1111} - a_{1122} - 2a_{111122} + a_{112211}$  and  $C_4 = a_{111111} + a_{111122} - a_{112211}$ , and  $\theta$  the angle between magnetization and current directions. This result is based on power expansions in terms of  $\cos^n\theta$ ; even though our data is analysed using the following expression:

$$\rho(\theta) = a_0 + a_u\cos 2\theta + a_c\cos 4\theta \quad (4)$$

since we can extract direct information on the uniaxial and cubic components of the anisotropic magnetoresistance. The  $a_0$ ,  $a_u$  and  $a_c$  constants are related to the previous ones by  $a_0 = C_0 + C_2/2 + 5/8C_4$ ,  $a_u = (C_2 + C_4)/2$  and  $a_c = C_4/8$ .

We fit the angular dependence of AMR using the expression of Eq. 4, obtaining the coefficients  $a_u$  and  $a_c$ , which are proportional to the uniaxial and cubic component respectively. These are plotted as a function of temperature for the three different samples and an applied field of 5 Tesla in Fig. 4. It can be noticed that the uniaxial component ( $a_u$ ) shows a non-monotonic temperature dependence with its minimum shifted towards lower temperatures

with increasing thickness. The cubic component ( $a_c$ ) shows a monotonic dependence with a continuous increase as the temperature is decreased. Wu et al. observed a similar behavior in (Ga,Mn)As films.<sup>36</sup> They consider the cubic component arising from the ferromagnetic order of the sample which is due to reduced thermal fluctuations of the spins as the temperature is decreased and as the spins become more aligned it is possible to observe higher order terms. They considered the uniaxial component to be dependent on the ferromagnetic order as well as on a superparamagnetic component (SPM) arising from bound magnetic polarons (BMP).

Since the characteristic features are similar for the three thin films, we focus our discussion on the 67 nm thick film sample. Figures 5(a) and 5(b) show the temperature dependence of the fitting coefficients ( $a_u$  and  $a_c$ ) obtained at fields 0.1, 0.5, 1, 5 and 14 Tesla. The uniaxial component shows a similar temperature dependence for all field values. Its magnitude increases with an increasing magnetic field above 140 K. Below 140 K we notice a non-monotonic field dependence in  $a_u$ . The increase in magnitude of  $a_u$  with magnetic field for  $T > 140$  K is contrary to the notion that AMR ( $\text{AMR}=(\rho_{\parallel} - \rho_{\perp})/\rho_{ave}$ ) is independent of the magnetic field at fields above the saturation field. This behavior can be explained on the basis that  $\text{Fe}_3\text{O}_4$  films contain APBs, which leads to a field dependent MR due to a non-saturation of the magnetization in fields up to several Tesla. The non-monotonic field dependence below 140 K could be related to the sign change of the magnetic anisotropy constant ( $K_1$ ) in magnetite, which happens above  $T_V$  at  $\sim 130$  K.<sup>42</sup> In contrast to it, the cubic component shows the same temperature dependence for all field values and no field dependence down to a temperature of about 200 K. Below 200 K  $a_c$  shows a different temperature dependence for different field values, with a stronger increase in magnitude for higher magnetic fields. At this moment we do not have a satisfactory explanation for this field dependency.

The fact that the additional symmetry appears at a temperature well above  $T_V$  is in agreement with previous reports where anomalies in muon spin rotation ( $\mu\text{SR}$ ) measurements<sup>43</sup> and neutron scattering experiments<sup>44,45</sup> have been observed at temperatures  $T > T_V+100$ , which have been related to the formation of polarons.

Recalling the discussion on the temperature dependence of the resistivity for our films, we consider the activation energies measured in region II. Following the model by Ihle et al.,<sup>32</sup> the electron-phonon coupling constant ( $S_0$ ) was obtained and the temperature of transition



between the SP band and hopping conduction region, was calculated using the expression  $kT' = \omega_0 \{2 \ln[2S_0 + (1 + 4S_0^2)^{1/2}]\}^{-1}$  <sup>46</sup>, where  $\omega_0 = 0.07eV$ . We obtained the temperature value of  $T' = 215K$  for the 67 nm thick film. This is in good agreement with the temperature where the  $a_c$  component shows the splitting with the field (see Fig. 5(b)) below some 200 K, suggesting that the observed anomaly is a consequence of a change in the conduction mechanism in magnetite due to the formation of polarons. Piekarczyk et al. <sup>47,48</sup> have recently proposed a mechanism for the Verwey transition as a cooperative effect between intra-atomic Coulomb interaction of Fe ions and phonon-driven lattice instability. They developed a model which shows that the strong electron-phonon coupling induces local crystal deformations and a polaronic short-range order above  $T_V$  and point out that the signs of the metal-insulator transition already appear at about 200 K. <sup>44,45,49</sup> According to their model, the  $X_3$  transversal optic phonon mode is responsible for the observation of charge-order stabilization at temperatures higher than the Verwey transition temperature, this mode consists of atomic displacements of the octahedral Fe and O atoms along  $\langle 110 \rangle$  and  $\langle 1\bar{1}0 \rangle$  directions in alternate planes. These displacements modify the interplanar distances between Fe-O atoms, stabilizing charge and orbital order of the  $t_{2g}$  states (see Fig. 6). The charge order creates a charge disequilibrium between the Fe ions on B sites (octahedrally coordinated cation sites in the spinel structure of magnetite), ideally departing from the average  $Fe^{2.5+}$  state to  $Fe^{2+}$  and  $Fe^{3+}$  at different octahedral sites. It is known that  $Fe^{3+}$  has a singlet ground state  ${}^6S_{5/2}$  with orbital moment zero and therefore no spin-orbit splitting. On the other hand the  $Fe^{2+}$  has a ground state  ${}^5D_4$  that will be split by spin-orbit interactions. <sup>50</sup> Therefore the charge ordering produces an enhancement of the effect of the spin-orbit interaction. Since the anisotropic magnetoresistance is a consequence of this interaction <sup>14,15,18</sup> it can be expected that the the effect of polaron formation, thus charge ordering in the system can be observed by anisotropic magnetoresistance measurements as evidence from our observations.

#### IV. CONCLUSION

In summary, we performed a study of the angular dependence of AMR for epitaxial  $Fe_3O_4$  films deposited on MgO (001) substrates and also on a (001)-oriented stoichiometric  $Fe_3O_4$  single crystal. It is shown that for temperatures below 200 K, the anisotropic magnetoresistance deviates from its normal  $\cos^2\theta$  angular dependence, this deviation is

manifested as an additional set of peaks at  $90^\circ$  and  $270^\circ$ . This observation is compared with the mechanism of the Verwey transition suggesting that the additional feature observed is related to a change in the conduction mechanism due to the formation of polaronic short-range order at temperatures above  $T_V$ . The effect of polaron formation can be observed by anisotropic magnetoresistance measurements as a consequence of spin-orbit enhancement induced by the charge order formation as explained above.

## V. ACKNOWLEDGEMENTS

Authors would like to gratefully acknowledge the financial support from the Science Foundation of Ireland (SFI) under Contract No. 06/IN.1/I91

- 
- <sup>1</sup> Y. Tokura and N. Nagaosa, *Science* **288**, 462 (2000).
- <sup>2</sup> M. Imada, A. Fujimori, and Y. Tokura, *Rev. Mod. Phys.* **70**, 1039 (1998).
- <sup>3</sup> M. Ziese, *Rep. Prog. Phys.* **65**, 143 (2002).
- <sup>4</sup> I. Žutić, J. Fabian, and S. D. Sarma, *Rev. Mod. Phys.* **76**, 323 (2004).
- <sup>5</sup> M. Fonin, Y. S. Dedkov, R. Pentcheva, U. Rüdiger, and G. Güntherodt, *J. Phys. Condens. Matter* **19**, 315217 (2007).
- <sup>6</sup> F. Walz, *J. Phys.: Condens. Matter.* **14**, R285 (2002).
- <sup>7</sup> S. K. Arora, H.-C. Wu, R. J. Choudhary, I. V. Shvets, O. N. Mryasov, H. Yao, and W. Y Ching, *Phys. Rev. B* **77**, 134443 (2008).
- <sup>8</sup> D. T. Margulies, F. T. Parker, F. E Spada, R. S Goldman, J. Li, R. Sinclair, A. E. Berkowitz, *Phys. Rev. B* **53**, 9175 (1996).
- <sup>9</sup> S. Kale, M. Bhagat, S. E. Lofland, T. Scabarozzi, S. B. Ogale, A. Orozco, S. R. Shinde, T. Venkatesan, R. Hannoyer, B. Mercey, et al., *Phys. Rev. B* **64**, 205413 (2001).
- <sup>10</sup> W. Eerenstein, T. T. M. Palstra, T. Hibma, and S. Celotto, *Phys. Rev. B* **68**, 014428 (2003).
- <sup>11</sup> R. G. S. Sofin, S. K. Arora, and I. V. Shvets, *J. Appl. Phys.* **97**, 10D315 (2005).
- <sup>12</sup> W. Eerenstein, T. T. M. Palstra, S. S. Saxena, and T. Hibma, *Phys. Rev. Lett.* **88**, 247204 (2002).
- <sup>13</sup> S. K. Arora, R. G. S. Sofin, and I. V. Shvets, *Phys. Rev. B* **72**, 134404 (2005).

- <sup>14</sup> J. Smit, *Physica* **16**, 612 (1951).
- <sup>15</sup> T. R. McGuire and R. I. Potter, *IEEE Trans. Mag.* **11**, 1018 (1975).
- <sup>16</sup> J. P. Jan, *Solid State Physics*, edited by F. Seitz and D. Turnbull **Vol. 5**, 1 (1957).
- <sup>17</sup> L. Berger, *Phys. Rev.* **138**, 1083 (1965).
- <sup>18</sup> R. I. Potter, *Phys. Rev. B* **10**, 4626 (1974).
- <sup>19</sup> I. A. Campbell, A. Fert, and O. Jaoul, *J. Phys. C: Solid State Phys.* **3**, S95 (1970).
- <sup>20</sup> I. Pallecchi, A. Gadaleta, L. Pellegrino, G. C. Gazzadi, E. Bellingeri, A. S. Siri, and D. Marré, *Phys. Rev. B* **76**, 174401 (2007).
- <sup>21</sup> V. S. Amaral, A. A. C. S. Loureço, J. P. Araújo, A. M. Pereira, J. B. Sousa, P. B. Tavares, J. M. Vieira, E. Alves, M. F. da Silva, and J. C. Soares, *J. Appl. Phys.* **87**, 5570 (2000).
- <sup>22</sup> K. I. Bolotin, F. Kuemmeth, and D. C. Ralph, *Phys. Rev. Lett.* **97**, 127202 (2006).
- <sup>23</sup> C. Ruster, C. Gould, T. Jungwirth, J. Sinova, G. M. Schott, R. Giraud, K. Brunner, G. Schmidt, and L. W. Molenkamp, *Phys. Rev. Lett.* **94**, 027203 (2005).
- <sup>24</sup> M. Viret, M. Gabureac, F. Ott, C. Fermon, C. Barreteau, G. Autes, and R. Guirado-Lopez, *Eur. Phys. J. B* **51**, 1 (2006).
- <sup>25</sup> M. Bibes, V. Laukhin, S. Valencia, B. Martnez, J. Fontcuberta, O. Y. Gorbenko, A. R. Kaul, and J. L. Martínez, *J. Phys. Condens. Matter* **17**, 2733 (2005).
- <sup>26</sup> M. Ziese and H. J. Blythe, *J. Phys: Condens. Matter* **12**, 13 (2000).
- <sup>27</sup> S. Sena, R. Lindley, H. Blythe, C. Sauer, M. Al-Kafarji, and G. Gehring, *J. Magn. Magn. Mater.* **176**, 111 (1997).
- <sup>28</sup> S. K. Arora, R. G. S. Sofin, I. V. Shvets, R. Kumar, M. W. Khan, and J. P. Srivastava, *J. Appl. Phys* **97**, 10C310 (2005).
- <sup>29</sup> M. Ziese and C. Sritiwarawong, *Phys. Rev. B* **58**, 11519 (1998).
- <sup>30</sup> N. F. Mott, *Conduction in Non-Crystalline Materials* (Clarendon Press, Oxford, 1993), p. 17ff.
- <sup>31</sup> S. B. Ogale, K. Ghosh, R. P. Sharma, R. L. Greene, R. Ramesh, and T. Venkatesan, *Phys. Rev. B* **57**, 7823 (1998).
- <sup>32</sup> D. Ihle and B. Lorenz, *J. Phys. C: Solid State Phys.* **19**, 5239 (1986).
- <sup>33</sup> M. Ziese, *Phys. Rev. B* **62**, 1044 (2000).
- <sup>34</sup> X. Jin, R. Ramos, Y. Zhou, C. McEvoy, and I. V. Shvets, *J. Appl. Phys.* **99**, 08C509 (2006).
- <sup>35</sup> J. O'Donnell, J. N. Eckstein, and M. S. Rzechowski, *Appl. Phys. Lett.* **76**, 218 (2000).
- <sup>36</sup> D. Wu, P. Wei, E. Johnston-Halperin, D. D. Awschalom, and J. Shi, *Phys. Rev. B* **77**, 125320

- (2008).
- <sup>37</sup> A. W. Rushforth, K. Vyborny, C. S. King, K. W. Edmonds, R. P. Champion, C. T. Foxon, J. Wunderlich, A. C. Irvine, P. Vasek, V. Novak, K. Olejnik, J. Sinova, T. Jungwirth, B. L. Gallagher, Phys. Rev. Lett. **99**, 147207 (2007).
- <sup>38</sup> M. Bibes, B. Martínez, J. Fontcuberta, V. Trtik, C. Ferrater, F. Sánchez, M. Varela, R. Hiergeist, and K. Steenbeck, J. Magn. Magn. Mater. **211**, 206 (2000).
- <sup>39</sup> W. Döring, Ann. Phys. **32**, 259 (1938).
- <sup>40</sup> R. P. vanGorkom, J. Caro, T. M. Klapwijk, and S. Radelaar, Phys. Rev. B **63**, 134432 (2001).
- <sup>41</sup> R. R. Birss, *Symmetry and Magnetism* (North-Holland Publishing Co. Amsterdam, 1964).
- <sup>42</sup> P. A. A. van der Heijden, M. G. van Opstal, C. H. W. Swüste, P. H. J. Bloemen, J. M. Gaines, and W. J. M. de Jonge, J. Magn. Magn. Mater. **182**, 71 (1998).
- <sup>43</sup> C. Boekema, R. L. Lichti, A. B. Denison, A. M. Brabers, D. W. Cooke, R. H. Heffner, R. L. Hutson, and M. E. Schillaci, Hyperfine Interactions **31**, 487 (1986).
- <sup>44</sup> S. M. Shapiro, M. Iizumi, and G. Shirane, Phys. Rev. B **14**, 200 (1976).
- <sup>45</sup> Y. Yamada, N. Wakabayashi, R. M. Nicklow, Phys. Rev. B **21**, 4642 (1980).
- <sup>46</sup> D. Ihle, Z. Phys. B **58**, 91 (1985).
- <sup>47</sup> P. Piekarz, K. Parlinski, and A. M. Olés, Phys. Rev. Lett. **97**, 156402 (2006).
- <sup>48</sup> P. Piekarz, K. Parlinski, and A. M. Olés, Phys. Rev. B **76**, 165124 (2007).
- <sup>49</sup> I. V. Shvets, G. Mariotto, K. Jordan, N. Berdunov, R. Kantor, and S. Murphy, Phys. Rev. B **70**, 155406 (2004).
- <sup>50</sup> R. J. McQueeney, M. Yethiraj, W. Montfrooij, J. S. Gardner, P. Metcalf, and J. M. Honig, Phys. Rev. B **73**, 174409 (2006).

Thickness (nm)	Arrhenius law (meV)		Small-polaron hopping (meV)	VRH (K)
	$\rho = \rho_{\infty} \exp(E_a/kT)$		$\rho/T^{3/2} = A \exp(W_p/kT)$	$\rho = \rho_{\infty} \exp(T_0/T)^{1/4}$
	$E_a^{II}$	$E_a^{III}$	$W_p^I$	$T_0$ (regime III)
33	58.0	92.5	53.0	$3.7 * 10^8$
67	56.8	102.9	52.6	$6.0 * 10^8$
200	55.0	106.9	46.1	$8.8 * 10^8$
single crystal	31.8	112.6	33.0	$9.1 * 10^8$

TABLE I: Values of activation energies ( $E_a$ ) and polaron hopping energies ( $W_p$ ) at 0 Tesla in different temperature regions determined using various conductivity models for different thickness films and single crystal magnetite.  $W_p^I$  relate to the temperature region  $T > 200$  K;  $E_a^{II}$  to the region  $120 \text{ K} < T < 200 \text{ K}$ .  $E_a^{III}$  and  $T_0$  were obtained at temperatures below the Verwey transition.

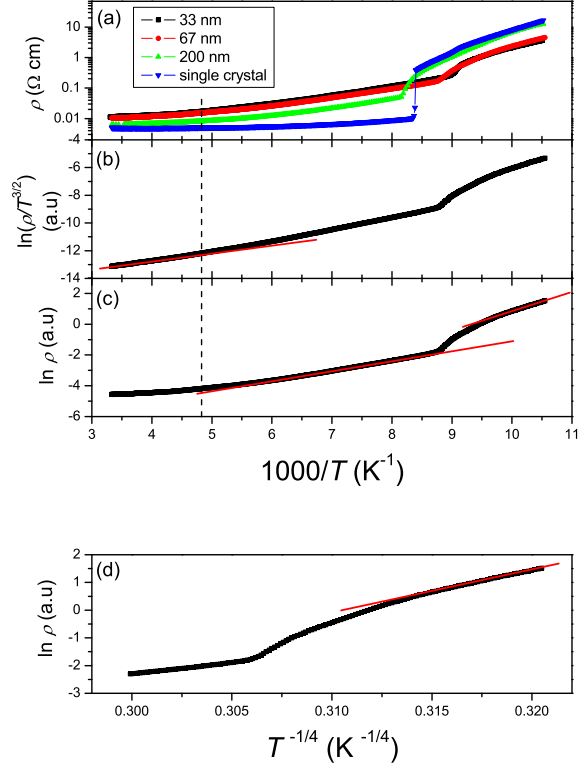


FIG. 1: (Color online) (a) Temperature dependence of the resistivity for all the thin film samples of Fe<sub>3</sub>O<sub>4</sub> along with that of single crystal Fe<sub>3</sub>O<sub>4</sub> samples. The Verwey transition temperatures are found to be 110, 112 and 121 K for the 33, 67 and 200 nm thick films respectively. Verwey transition for the single crystal was 119 K. Panels (b) to (d) show the resistivity of the 67 nm thick film fitted (red lines) to the (b) Small-polaron hopping (c) Arrhenius law and (d) variable range hopping (VRH) models. The VRH expression is only fitted for temperatures below  $T_V$ .

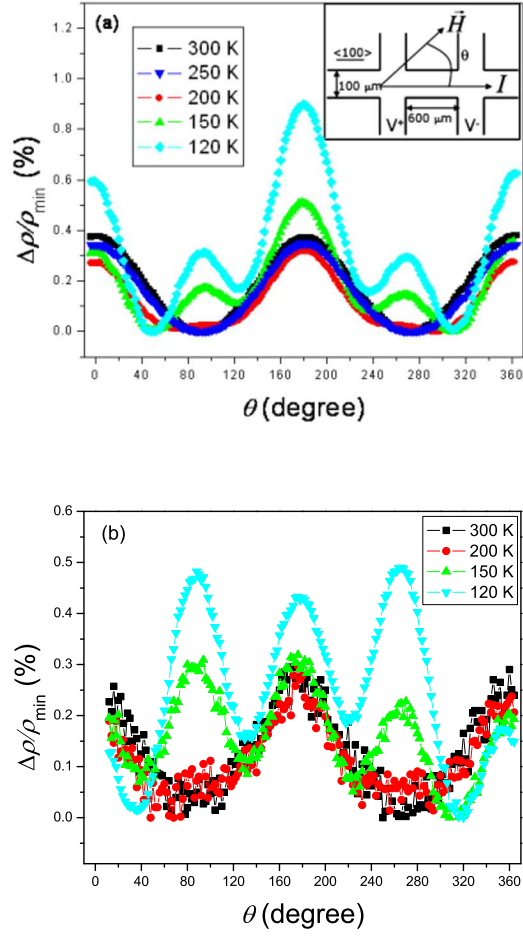


FIG. 2: (Color online) (a) Angular dependence of the magnetoresistance for the 67 nm Fe<sub>3</sub>O<sub>4</sub> thin film sample measured at  $\mu_0\vec{H}=5$  Tesla. Below 200 K, it can be seen that the additional anisotropy develops with peaks at 90° and 270°. (b) Angular scan of AMR at different temperatures for the (001) oriented single crystal Fe<sub>3</sub>O<sub>4</sub> measured at 5 Tesla field. Inset in Fig. 2(a) shows the Hall bar geometry used in these investigations.

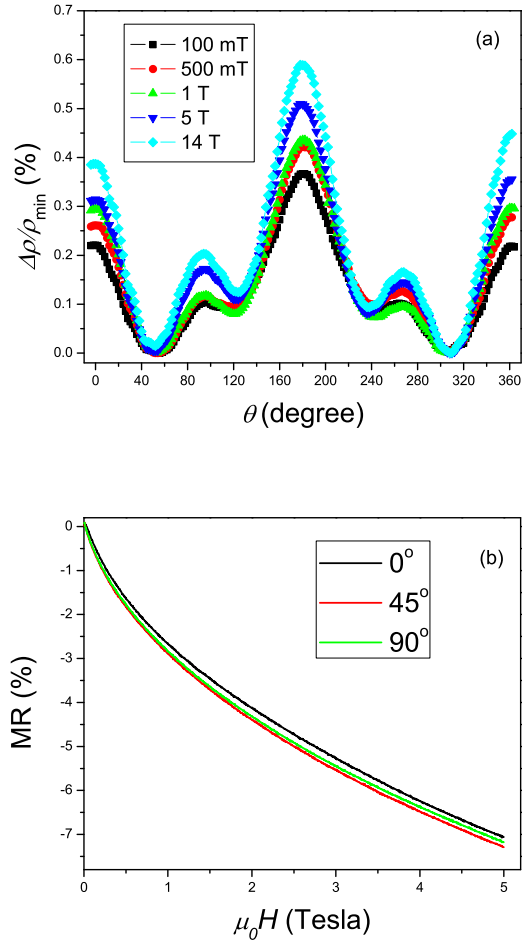


FIG. 3: (Color online) (a) Angular dependence of the magnetoresistance for the 67 nm thick  $\text{Fe}_3\text{O}_4$  thin film measured at 150 K. The data is plotted for different field values of 100 mT, 500 mT, 1 T, 5 T and 14 T (b) Magnetoresistance of the 67 nm thick film measured at field orientations 0, 45 and 90 ° with respect to the current.



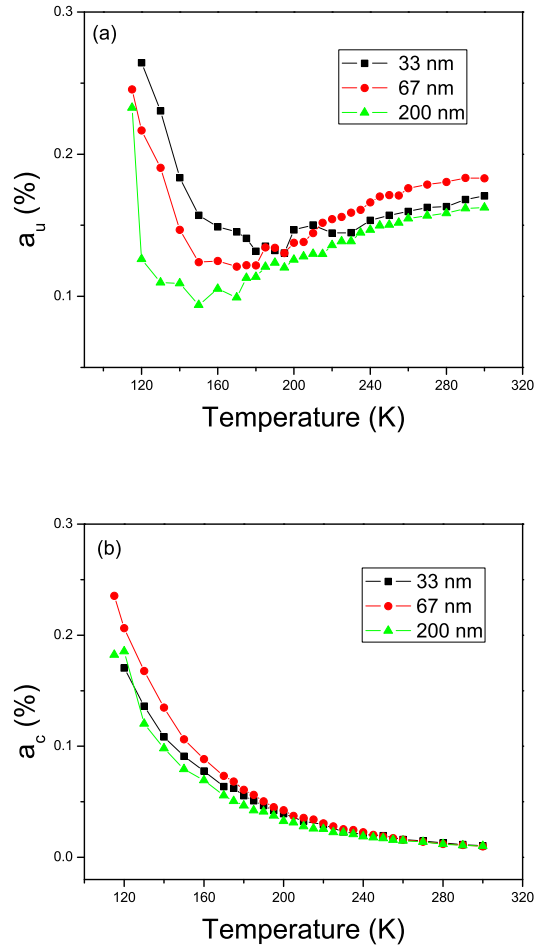


FIG. 4: (Color online) Temperature dependence of the (a) uniaxial ( $a_u$ ) and (b) cubic ( $a_c$ ) components for samples of three different thicknesses. The coefficients are determined from the angular-dependent AMR scans taken at each temperature with an applied field of 5 Tesla.

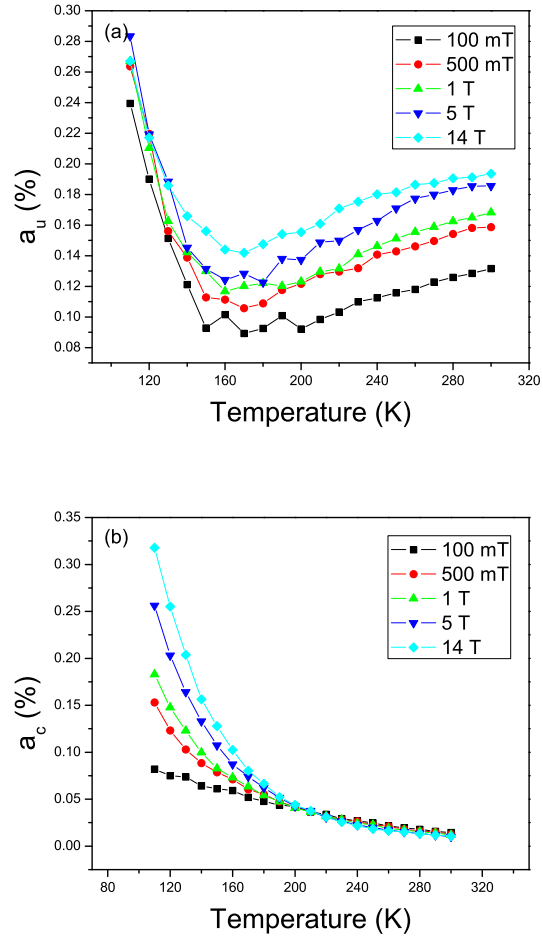


FIG. 5: (Color online) Temperature dependence of the (a) uniaxial ( $a_u$ ) and (b) cubic ( $a_c$ ) components at different applied fields for the 67 nm thick film.

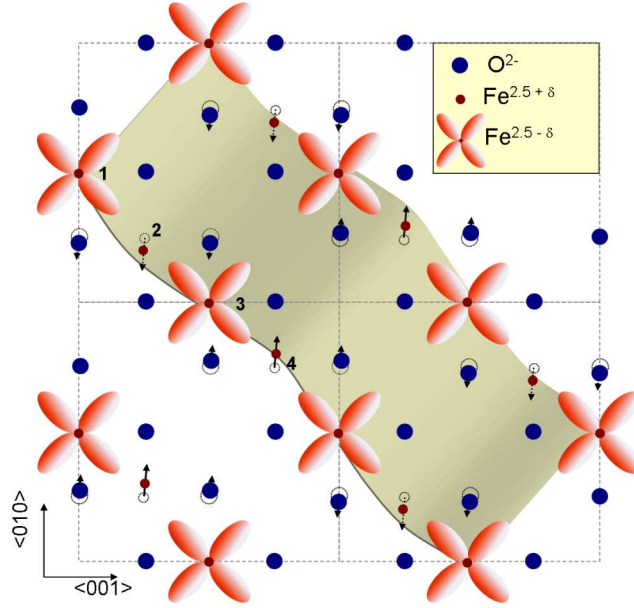


FIG. 6: (Color online) Representation of the atomic displacements induced by the  $X_3$  phonon mode. Broken (solid) arrows represent displacements along  $\langle 1\bar{1}0 \rangle$  ( $\langle \bar{1}10 \rangle$ ). The cations in positions 2 and 4 and its nearest neighbor anions in the  $\langle 001 \rangle$  direction are displaced along  $\langle 1\bar{1}0 \rangle$  ( $\langle \bar{1}10 \rangle$ ) respectively, therefore the atomic sites in positions 1 and 3 will present  $t_{2g}$  orbital ordering ( $d_{yz}$  orbital) due to the lower Coulomb repulsion as a consequence of the out of plane displacement of two of the nearest neighbor anions.